Return current in hysteretic Josephson junctions: Experimental distribution in the thermal activation regime

M. G. Castellano[a] and G. Torrioli
INFN and Istituto di Elettronica dello Stato Solido–C.N.R., Via Cineto Romano 42, 00156 Roma, Italy

F. Chiarello and C. Cosmelli
INFN and Dipartimento di Fisica, Università La Sapienza, Piazzale A. Moro 5, 00185 Roma, Italy

P. Carelli
INFM and Università dell'Aquila, Monteluco di Roio, 67040 L'Aquila, Italy

(Received 8 December 1998; accepted for publication 2 September 1999)

We present an experimental study on the retrapping process of a hysteretic, high-quality Josephson junction; namely, we have measured the distribution of the values at which the junction switches back from the voltage state to the zero-voltage state, as a function of the applied magnetic field. While the opposite process (escape from the zero-voltage state) has been extensively studied in the past, both from the theoretical and the experimental point of view, little is found in the literature on the retrapping process. In terms of the tilted washboard potential, the process corresponds to the retrapping from the running state to a locked state in a potential well. The interest of the measurements is in the fact that the value of the return current can be directly related to the dissipation in the junction. While the deterministic behavior, experimentally measured through the $I-V$ curve, appears to be in agreement with the theoretical predictions, even in minor details, the statistical behavior is strongly different from what is expected. The disagreement is found even in zero-applied magnetic field and it cannot be attributed to external noise in the system. From the experimental statistical properties, we find values for the effective dissipation much lower than those obtained from the deterministic curves, a result which could be of interest in experiments on the observation of macroscopic quantum phenomena. © *1999 American Institute of Physics.* [S0021-8979(99)08123-2]

I. INTRODUCTION

To identify which equivalent resistance is responsible for the intrinsic dissipation of a Josephson junction, several different approaches can be used. It is possible to analyze the $I-V$ characteristics to determine several parameters which are related to different damping and excitation phenomena in the junctions: the normal resistance, which refers to the normal-state behavior, the subgap resistance, or its differential value determined by the quasiparticle conductance. By comparing the experimental $I-V$ curve with the theory,[1] either with a simple resistively shunted junction (RSJ) model, or with a more refined model such as the quasiparticle tunneling model (QPT), it is possible to infer the value of the resistance responsible for the dissipation.[2]

As an alternative, one can study the process of escape from the zero-voltage state[3] (when the junction jumps from the Josephson part of the $I-V$ characteristic to the other branch) or the opposite process, the return from the running state (voltage different from zero) to the zero-voltage state.[4] Actually, as far as the dissipation is concerned, the escape process gives information only if the junction is in a particular regime of damping, otherwise the friction coefficient does not influence the distribution; the return process, instead, is always dependent on the dissipation.

In this article we analyze the return current distribution for a high-quality Nb/AlO_x/Nb Josephson junction to get the effective dissipation involved in the process, at liquid-helium temperature. A constant magnetic field is applied to the junction in order to vary the critical current value and then study the junction in different regimes and conditions.

II. ESCAPE FROM AND RETURN TO THE ZERO-VOLTAGE STATE

The two processes can be understood by referring to the well-known mechanical analog, which depicts the dynamics of the Josephson junction as that of a particle of mass $C(\Phi_0/2\pi)^2$ [where C is the junction capacitance and $\Phi_0 = h/2e$ is the flux quantum], with dissipation $(\Phi_0/2\pi)^2\,1/R$ (where R is the junction resistance), described by a mechanical degree of freedom δ (the phase difference across the junction) and subjected to a tilted washboard potential U:

$$U(\delta) = -\frac{\Phi_0}{2\pi} I_c \left(\delta \frac{I}{I_c} + \cos(\delta) \right). \tag{2.1}$$

Here, I_c is the junction critical current and I is the current bias. In the escape process, the particle is initially trapped in a potential metastable well, oscillating at the plasma frequency. When the potential slope is increased to a certain level (by increasing the current bias of the junction), the fluctuations make it possible for the particle to roll over the potential barrier (or tunnel through, in the quantum regime)

[a]Electronic mail: castellano@iess.rm.cnr.it

and run down the potential. The current value at which this occurs, in the absence of noise and fluctuations, is the critical current I_c.

In the return process, the particle is running while the potential slope is being decreased. When the energy dissipated by the friction (modeled as an equivalent resistance R_j, in parallel with the junction, which is not necessarily coincident with that used in the RSJ model) equals the kinetic energy, the particle stops in one of the potential wells. The corresponding current value is the (noiseless) return current I_r.

These processes are intrinsically stochastic, since they are activated by thermal or quantum fluctuations, as well as by ambient noise: the fluctuations increase the value of the return current (and decrease the value of the escape current) with respect to the deterministic value. The distribution of values is asymmetric: for the escape process, which is upper bounded by the noiseless I_c, the sharper side is at values larger than the mean value; for the return process the opposite is true, since the noiseless I_r is a lower bound. The experiment consists in sweeping the junction with a current ramp, at a rate dI/dt, collecting the current values at which escape or return occur, and comparing the resulting histogram with the theory.

Regarding the escape from the zero voltage, the analysis is performed following the well-known approach of Ref. 5. The switching out from the zero-voltage state can be modeled very simply as a thermal escape process from a metastable potential well, if $kT > \hbar\omega(I)/7.2$, $\omega(I)$ being the frequency of the small oscillations in the potential well. According to Kramers,[6] the lifetime τ of the zero-voltage state, at a bias current I, can be expressed in terms of the thermal activation energy kT and of the energy barrier to overcome $\Delta U(I)$:

$$\tau^{-1}(I) = A \exp\left[-\frac{\Delta U(I)}{kT}\right]. \tag{2.2}$$

The prefactor $A = a_t \omega(I)/2\pi$ is related to the attempt frequency; a_t is a factor depending on the details of the damping regime (for highly hysteretic junctions, the regime of interest is intermediate or low damping).[7,8] Our junctions fall in the intermediate regime, with $a_t \approx 1$. The energy barrier

$$\Delta U \approx \frac{2\sqrt{2}}{3\pi}\Phi_0 I_c (1 - I/I_c)^{3/2}, \tag{2.3}$$

depends only on the bias and the critical currents; the dependence on $(I - I_c)^{3/2}$ derives from the RSJ model.

The expected theoretical distribution $P(I)$ is implicitly defined through the recursive relation

$$P(I) = \tau^{-1}(I)\left(\frac{dI}{dt}\right)^{-1}\left(1 - \int_0^I P(u)\,du\right). \tag{2.4}$$

Equation (2.4) gives a link between the two quantities $P(I)$ and $\tau(I)$, because the probability of having a switching in an interval dI around a bias value I is the product of two terms: the probability that the junction has not yet switched for smaller values of I [term $1 - \int_0^I P(u)\,du$], and the probability of switching in a time interval dt, which is given by the inverse lifetime $\tau^{-1}(I)$ times dt.

The analysis provides a check of the validity of the cubic approximation for the potential barrier, and allows us to get the effective temperature $T_{\rm esc}$ responsible for the escape process and the noiseless value of I_c. In the thermal regime, like in our case, $T_{\rm esc}$ should be coincident with the thermodynamic temperature, unless extra noise affects the system. A measurement of this process, then, gives an estimate of the effective temperature of the junction, as far as noise is concerned.

As regards the analysis for the return process, one can gather information both from the value of the return current and from the shape of the histogram. The first approach, where the measured value of I_r can be related directly to an effective dissipation R_j, is the most commonly found in the literature; indeed, a mention of measurements on the current distribution, due to thermal fluctuations, is found only in Ref. 4. By considering the overall energetic balance in the return process, a simple relationship links R_j and the value of the bias current at which the retrapping occurs:

$$I_r = \frac{4I_c}{\pi\omega(I)R_jC} \simeq \frac{4I_c}{\pi\omega_p R_j C}, \tag{2.5}$$

where $\omega_p = \sqrt{2\pi I_c/\Phi_0 C}$ is the junction plasma frequency. Actually, in this equation (and in the following) I_r refers to the noiseless value of the return current, which does not take into account the spread of the values due to thermal excitations. Experimentally, instead, we observe the current value at which the probability distribution is maximum, or at most the entire histogram of the current values: this sets an upper limit for the noiseless I_r but does not allow a precise determination, unless we use some model for investigating the retrapping process.

The relationship between the junction parameters and the histogram of the return current values has been studied by Ben-Jacob *et al.*[9] in the thermal regime, and by Chen, Fisher, and Leggett[1] in both thermal and quantum regimes with the constraint $I - I_r \ll I_r$.

Ben-Jacob *et al.* calculate the lifetime τ_r of the nonequilibrium state of the junction (running state) until it undergoes a transition to the zero-voltage equilibrium state. The dynamic equation they find is similar in form to that obtained by Kramers to describe the transition from a stable equilibrium state, although the two processes are very different, the return process being the transition from a stable nonequilibrium steady state. The lifetime in the return process has then the expression

$$\tau_r = R_j C \sqrt{\frac{\pi kT}{\Delta W}} e^{\Delta W/kT}, \tag{2.6}$$

where $\Delta W = (I - I_r)^2 R_j^2 C$. In a typical ramping experiment, in which the junction is swept by a decreasing current ramp, the distribution of the current values $P(I)$ is related to the lifetime according to Eq. (2.4).

Compared to the analysis of the escape process from the zero-voltage state, here the process involves critically three

TABLE I. Characteristics of the junctions at 4.2 K and zero-applied magnetic field.

J_c A/cm^2	side μm	I_c μA	R_n Ω	V_m mV	C pF	ω_p rad/s
100	4	16	80	35	0.8	2.5×10^{11}

parameters (I_r, R_j, T_r) instead of two (I_c, $T_{\rm esc}$). Unfortunately, the shape of an experimental distribution can be reconstructed by varying just two parameters, the third parameter giving only minor variations which fall in the range of the experimental errors. For the analysis of the return distribution, then, it is advisable to have an independent good knowledge of one parameter. In the thermal regime, where thermal fluctuations dominate, we can safely assign a value to the temperature, since it can be measured independently with an experiment of switching out from the zero-voltage state, excluding the presence of extra noise affecting the junction.

A deterministic evaluation of the $I-V$ characteristics in the return region and of its statistical properties is given by Chen, Fisher, and Leggett,[1] hereafter, cited as CFL. The CFL theory covers the parameter range where $I-I_r \ll I_r$, in the two limits of low temperature ($kT \ll \hbar\omega_p$) and high temperature ($\hbar\omega_p \ll kT$). In either limit, the square of the full width at half maximum of the distribution is given, within logarithmic factors, by the following formula:

$$\sigma^2(T) = \text{const}\ \mu\ f(T) \simeq \text{const}\ \frac{\hbar\omega_p}{I_c\Phi_0} I_r^2, \tag{2.7}$$

where the constant is if order 1, $f(T)$ is a function which tends to 1 as T tends to 0 and is proportional to T in the limit of high T. $\mu = \hbar\omega_p / I_c\Phi_0$ gives a measure of the overall importance of quantum fluctuations with respect to the classical dynamics of the junction, and it is usually much less than 1. Formula (2.7) has the inconvenience of being expressed explicitly in terms of the noiseless I_r, which, as noted before, must be extracted from the data by using some model.

We will consider again the quantities above and the relationships among them in the discussion of the measurements.

III. EXPERIMENTAL SETUP

Our junctions are high-quality Nb/AlO_x/Nb trilayer tunnel junctions. The trilayer (base electrode 1800 Å, aluminum layer 70 Å, top electrode 1000 Å thick) is deposited onto a nonoxidized silicon wafer, 111 oriented; the layout is defined by lift-off through a photoresist mask. The junctions have a window geometry of 4 μm side, defined by reactive ion etching of the top electrode and self-aligned SiO insulation.[10] The wiring layer is again niobium, 4000 Å thick. The junction quality is evaluated by means of the factor V_m, that is, the product of the critical current times the static resistance at 2 mV, without any correction for the strong coupling effect—which would increase the V_m. The junction characteristics at 4.2 K are collected in Table I.

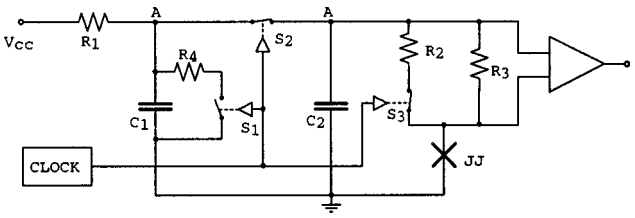

FIG. 1. Scheme of the electronic apparatus.

The junction was put inside a copper holder,[11] which provided a $R-C-R$ filtering stage at low temperature for all the leads (phosphor–bronze twisted pairs). A solenoid placed rigidly around the chip holder provided a magnetic field (parallel to the junction plane and in-line with one side of the junction), which could be varied to modulate the Josephson current. The whole insert is immersed into a liquid-helium bath, to ensure the proper thermalization of the device.

The switching of the junction (from or towards the zero-voltage, locked state) was measured as follows. The junction was swept by a current ramp, varying with a known derivative. The voltage across the junction was sent to a comparator: once the threshold corresponding to the selected jump was reached, the comparator sent a trigger signal to the data acquisition system, so that the corresponding current value was recorded. The data were collected into histograms and analyzed.

Measurements of the switching currents for the escape and the return processes require two contrasting characteristics of the electronic system which reads the current values: high sensitivity (to resolve the values in the narrow distributions of I_c or I_r), and in the meantime high dynamic range (since the junction must follow the entire $I-V$ path, from I_c to zero). These problems are more evident for the return current, where both the mean value and the distribution spread are very small.

We developed an electronic setup that allows accurate measurements of the return current. The current sweep is given by the discharge current of a capacitor, to avoid any unwanted effects due to the quantization of digital generators. The current is read by the voltage through a large resistor, to achieve high sensitivity. This, however, limits heavily the maximum amount of current that can be fed to the junction, which instead must be driven over the gap region in order to go through the whole hysteresis cycle. To overcome the problem, we envisaged a system of electronic switches (Fig. 1) that allows us to use two different resistors, a smaller one when the current increases and a larger one when the current goes back to zero.

The analog switches can be driven open or shorted by a clock signal as it follows. At first, S_1 is opened while S_2 and S_3 are shorted, consequently, the voltage at point A increases towards $V_{cc}R_p/(R_1+R_p)$, where R_p is the parallel of R_2 and R_3, and the capacitors C_1 and C_2 are charged. The time constant for the buildup of the current is set at a small value, to shorten the run time; the current is read through the voltage across R_p. In the second step, S_1 is shorted while S_2 and S_3 are opened. Here, C_1 is slowly discharged through R_4 and C_2 through the series of R_3 with the junction. The current

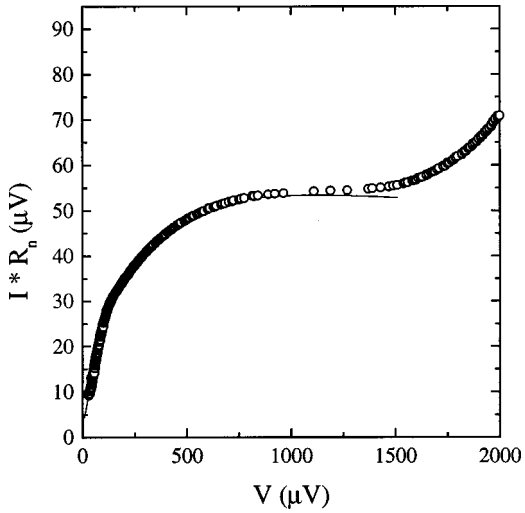

FIG. 2. Experimental $I-V$ quasiparticle branch (open circle) and its fit with the BCS model (line); the fit parameters are 1.325 mV for the gap voltage and 4.2 K for the temperature.

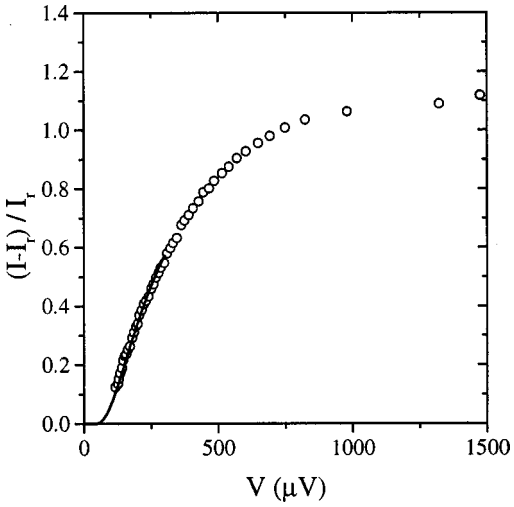

FIG. 3. Experimental $I-V$ quasiparticle branch (open circle) and its fit with the Chen–Fisher–Leggett model close to the retrapping point (line).

flowing through the junction is then read by measuring the voltage across R_3, whose chosen value is large in order to improve the sensitivity. To further magnify the current distributions, we added a proper dc voltage offset to keep the value of the switching current close to zero and then we sent this signal to a limiter, which provided a further gain of 20–50 for signals inside the range of about 150 μV, while keeping the overall dynamic signal inside the range of the acquisition system. With a suitable choice of R_2 and R_3 this setup allowed us to collect current distributions with a channel resolution of 1.5 pA for the return current and 42 pA for the escape current. This electronic setup can be used also for measurements of the escape process. In this case, the current buildup must be slower by changing the time constant.

IV. *I– V* CHARACTERIZATION

At first, the $I-V$ characteristics of the junction in a liquid-helium bath have been recorded and analyzed according to the BCS model,[12] to check the behavior of the subgap part and to get the value of the gap. In our case the best fit, shown in Fig. 2, gives $V_g=1.325$ mV at 4.2 K and the agreement with the expected behavior is good.

The value of the plasma frequency at zero-applied magnetic field is either calculated from the formula $\omega_p=\sqrt{2\pi I_c/\Phi_0 C}$, using a previous estimate of C (from Fiske steps), or from a fit of the $I-V$ characteristic close to the return value[1] with the formula

$$\frac{I-I_r}{I_r}=\left(\frac{AV_0}{V}+B\right)e^{-V_0/V}, \tag{4.1}$$

where A and B are constants usually of the order of unity. From the fit of the data it is possible to get V_0, which is given by $V_0=\omega_p\Phi_0$, and hence, ω_p. The major difficulty is in the determination of I_r; we decided to use as a first estimate the value at which the switching histograms are maximum (most probable observed value). This considered, the agreement between the CFL curve and the experimental data is quite good, as shown in Fig. 3; the calculated plasma frequency of $\omega_p=2.5\times10^{11}$ rad/s is in agreement (within 20%) with the value found from the fit. With this value, one gets $\hbar\omega_p/k\simeq1.8$ K, which is not far from the bath temperature; according to CFL, the junction is in between the high- and low-temperature limits. By increasing the applied magnetic field to reduce the critical current, the junction moves towards the high-temperature regime.

Figure 4 shows the behavior of the critical and of the return current as a function of the applied magnetic field. The values of I_c are the noiseless values, as found from the analysis of the escape histograms (discussed in the next section); as regards I_r, we used as a first estimate the mean values of the switching distribution. The Josephson current follows the typical diffraction pattern; the continuous line is the usual $|\sin(x)/x|$ function. From the first zero, a London length of 1000 Å is found, and a corresponding Josephson length of 35 μm, which states that the junction can be considered small. The return current is also modulated by the

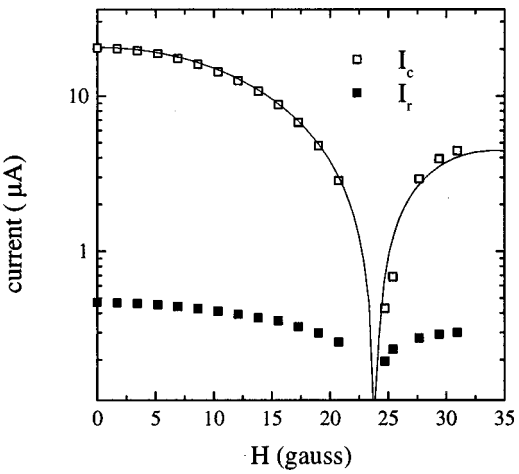

FIG. 4. Experimental critical and return current as a function of magnetic field; the continuous line is the theoretical pattern.

applied magnetic field; the CFL formula predicts a weak dependence such as $I_r \propto \sqrt{I_c}$, which fits the experimental points.

We can summarize the situation up to this point by stressing that the experimental observations on the $I-V$ characteristic show a good agreement with the expected behavior.

V. HISTOGRAM ANALYSIS

For any magnetic-field value, we measured, in two separate runs, the current value distributions for the process of return to the zero-voltage state and for the escape from the zero-voltage state. The switching out from the zero-voltage state allows a measurement of the noiseless critical current and of the effective temperature T_{esc} responsible for the process. The measured T_{esc} is, for all the values of the magnetic field, equal to the thermodynamic temperature within the experimental error. The only data points which would require further analysis are those close to the maximum depression of the Josephson current: at these values of the field, indeed, the junction is much less hysteretic than in other cases, so that the regime to be considered is no longer the purely underdamped one. Hence, from the escape measurements we can state that our system is not affected by extra noise.

In the return process, approaching the retrapping, some extra power is dissipated in the quasiparticle system (of the order of hundreds of pW). This power is then transmitted to the underlying substrate by phonons. At lower temperatures (on the order of hundreds of mK) and if the sample is in vacuum, the electron and phonon baths are no longer well coupled, so that their temperatures can be very different; this is the well-known hot-electron effect.[13] However, at our working temperature (4.2 K) this effect is completely negligible, even more so since the sample is immersed in liquid helium, which provides the necessary thermalization to the chip. This considered, and having excluded the presence of extra noise from the previous measurements, in the analysis of the return histogram we can be confident in setting the temperature equal to the liquid-helium temperature. A confirmation of the system temperature comes from an examination of the $I-V$ characteristics of Fig. 2. Setting the temperature equal to 4.2 K allows us to eliminate one free parameter from the fitting curve in the return histogram, reducing the total number of parameters to 2. In passing, we note that according to the theory an increase of the temperature in the retrapping process would lead to an enlargement of the histograms.

Let us now discuss the process of return to the zero-voltage state. Some of the histograms, normalized so as to have a unit area (with the current measured in microamperes), are collected in Fig. 5 for several values of the applied magnetic field. By increasing the magnetic field, the mean value of the histogram moves to lower current values, as expected, and the width spreads. The standard deviation σ of the experimental distribution is shown in Fig. 6 as a function of the magnetic field; in Fig. 6, for comparison is also displayed the modulation pattern of the critical current. Points corresponding to the same value of the critical current, on either side of the current pattern, should have the same behavior, disregarding the absolute value of the magnetic field; indeed, for these points σ is the same, showing that the magnetic field has an influence only through I_c and I_r. In the following, then, we will plot the measured quantities against the noiseless critical current value, instead of the magnetic field, keeping in mind that the higher I_c values correspond to the smaller magnetic-field values. The sudden decrease of σ at about 24 G is probably due to the junction entering a different dissipation regime, because of the large suppression of the Josephson current.

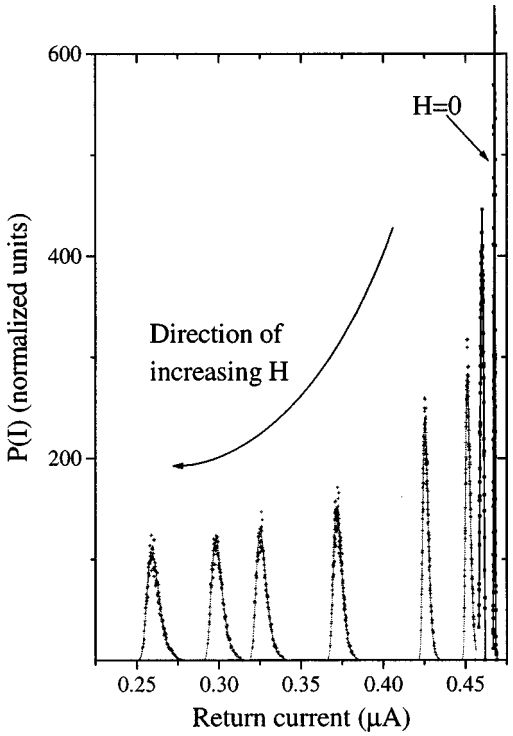

FIG. 5. Histograms of the return current values in the retrapping process, at the variation of the applied magnetic field. The line labeled *H* is used only to indicate the direction of increasing field. As the magnetic field is enhanced, the histogram center goes to a lower current value and the width spreads up.

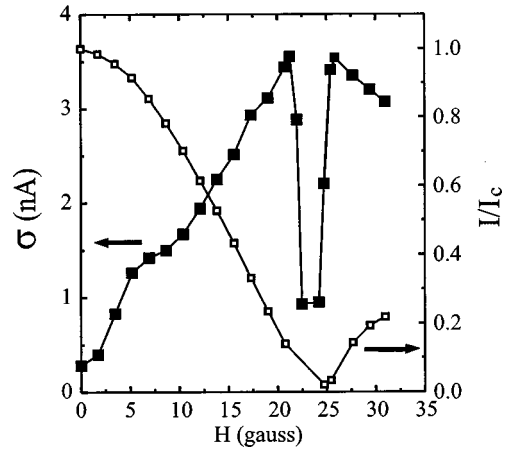

FIG. 6. Standard deviation of the experimental distribution of the return current (solid squares) vs applied magnetic field. For comparison, the critical current modulation curve (open squares) is also reported.

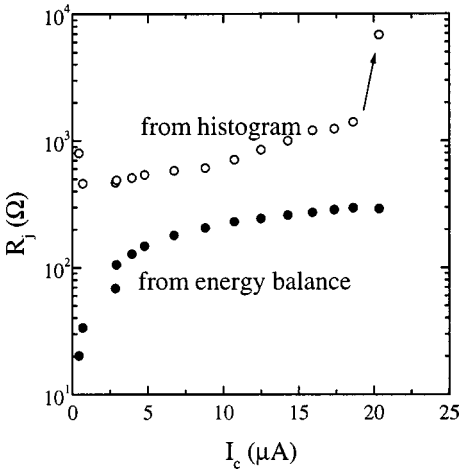

FIG. 7. Effective resistance vs applied magnetic field, calculated by energy balance considerations (filled dots) and from the histogram width (open dots).

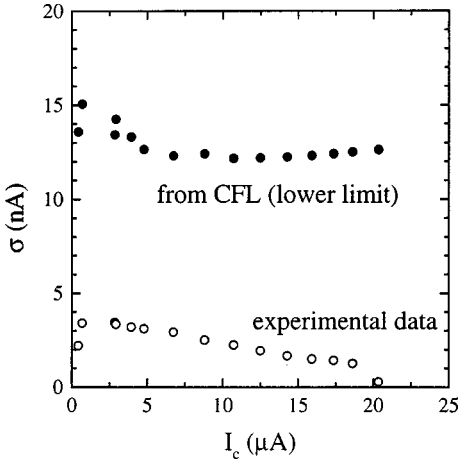

FIG. 8. Standard deviation of the return current distribution as a function of the critical current value, by applying a magnetic field. Open dots are the experimental points, while filled dots represent Eq. (2.7) with const=1 and $f(T)=1$, to give a lower limit.

The narrowest distribution width is found at zero-applied magnetic field, where $\sigma=0.28$ nA, which is the limit of our setup; in this case, the histogram turns out to be symmetric, since it is dominated by the intrinsic, Gaussian noise of the apparatus. The measured σ is then only an upper limit for the real width of the distribution. When the magnetic field is increased, the distribution width broadens and the histogram shape becomes asymmetric, as expected.

By analyzing the histogram according to the model of Ref. 9, and except for the low-field data, we find a good agreement between the data and the theoretical curve, and we can get the noiseless value of the return current and the effective resistance. As a matter of fact, the continuous lines in Fig. 5 are the theoretical fits of the experimental data.

Figure 7 displays (open points) the values of the effective resistance R_j found with this method, as a function of the (noiseless) critical current value. At low magnetic field, where I_c attains its maximum value, as already mentioned the histogram is dominated by the noise of our setup, so that the analysis of the distribution is misleading. However, it gives a lower limit for the effective resistance. We reported in Fig. 7 only the point at zero magnetic field, where $R_j > 6.8$ kΩ; the arrow shows the trend for the points in the region. This sudden increase cannot be explained either by additional noise terms (which, moreover, were not observed in the escape distributions made in the same conditions), or by the presence of the magnetic field, which was close or equal to zero. On the other extreme of the curve, at very low I_c, the reduction of the hysteresis probably makes the junction enter a different dissipation regime. In this region, we remark that the histogram width was still meaningful, because it was close to, but still larger than, our experimental limit.

Figure 7 shows for comparison the values of the effective resistance as obtained from the energy balance Eq. (2.5) (curve with filled dots). In this calculation we used the noiseless value of the I_r distribution, as obtained from the Ben-Jacob model. Using the mean value of the histogram as a better estimate of I_r would not alter the result very much, since the two quantities differ at most by 30%, in the reliable region where I_c is not too small. While the general behavior of the two curves looks similar, the disagreement in the absolute value is about a factor 10, the dissipation calculated by deterministic parameters being the higher one. Hence, the study of the distribution width leads to the conclusion that the dissipation is much lower than expected.

As an independent check, we compared the experimental width with the prediction of Eq. (2.7). In Fig. 8, the standard deviation of the experimental distribution is reported, together with a lower limit for Eq. (2.7), obtained by inserting the measured parameters and taking constant and $f(T)$ equal to unity (their lower bound). Once again, the experimental values are much smaller than expected. Again, the disagreement is more evident in the absence of applied magnetic field.

VI. CONCLUSIONS

We studied the effective dissipation of Nb/AlO_x/Nb tunnel junctions in the process of return to the zero-voltage state, performing extensive measurements of the statistical properties of the process, in the presence of an applied magnetic field.

While the deterministic behavior of the junction is in agreement with the theory, we found a severe inconsistency between the values of the effective dissipation as obtained from the deterministic parameters (such as the value of the retrapping current or the $I-V$ characteristic) and from the stochastic distribution of the retrapping values in the thermal regime. The effective resistance found with the latter analysis is higher by about a factor 10, leading to an unexpectedly low dissipation factor. We remark that most of the measurements found in the literature obtain the value of the dissipation from the deterministic characteristic, so that comparison with our data is not possible. This result could be relevant for those experiments which rely heavily on the low dissipation of Josephson devices to study macroscopic quantum effects. In particular, the experimental observation of macroscopic

quantum coherence (MQC) in rf superconducting quantum interference devices could be hindered, if not totally prevented, by the intrinsic dissipation in the junction; our result represents a further hope regarding the possibility of performing the measurement in a real junction.

ACKNOWLEDGMENTS

The authors gratefully acknowledge discussions with R. Cristiano, A. J. Leggett, P. Silvestrini, and A. Ustinov. This work has been supported by INFN under the MQC project.

[1] Y. C. Chen, M. P. A. Fisher and A. J. Leggett, J. Appl. Phys. **64**, 3119 (1988).
[2] R. Cristiano, L. Frunzio, C. Nappi, M. G. Castellano, G. Torrioli, and C. Cosmelli, J. Appl. Phys. **81**, 7418 (1997).
[3] J. M. Martinis, M. H. Devoret, and J. Clarke, Phys. Rev. B **35**, 4682 (1987).
[4] J. R. Kirtley, C. D. Tesche, W. J. Gallagher, A. W. Kleinsasser, R. L. Sandstrom, S. I. Raider, and M. P. A. Fisher, Phys. Rev. Lett. **61**, 2372 (1988).
[5] L. D. Jackel, W. W. Webb, J. E. Lukens, and S. S. Pei, Phys. Rev. B **9**, 115 (1974); T. A. Fulton and L. N. Dunkleberger, *ibid.* **9**, 4760 (1974).
[6] H. A. Kramers, Physica (Utrecht) **7**, 284 (1940).
[7] M. Büttiker, E. P. Harris, and R. Landauer, Phys. Rev. B **28**, 1268 (1983).
[8] P. Silvestrini, S. Pagano, R. Cristiano, O. Liengme, and K. E. Gray, Phys. Rev. Lett. **60**, 844 (1988).
[9] E. Ben-Jacob, D. J. Bergman, B. J. Matkowski, and Z. Shüss, Phys. Rev. A **26**, 2805 (1982).
[10] A. Shoji, F. Shinoki, S. Kosaka, M. Aoyagi, and H. Hayakawa, Appl. Phys. Lett. **41**, 1097 (1982).
[11] M. G. Castellano, R. Leoni, G. Torrioli, F. Chiarello, C. Cosmelli, A. Costantini, G. Diambrini-Palazzi, P. Carelli, R. Cristiano, and L. Frunzio, J. Appl. Phys. **80**, 2922 (1996).
[12] R. Cristiano, L. Frunzio, and C. Nappi, Nuovo Cimento D **14**, 395 (1992), and references therein.
[13] F. C. Wellstood, C. Urbina, and J. Clarke, Appl. Phys. Lett. **54**, 2599 (1989).